Received: 9 May 2022 | Revised: 7 November 2022 | Accepted: 11 November 2022

DOI: 10.1002/hbm.26161

RESEARCH ARTICLE

WILEY

The cortical regions and white matter tracts underlying auditory comprehension in patients with primary brain tumor

Jie Zhang[1,2,3,4,5] | Ye Yao[6,7,8] | Jin-song Wu[1,2,3,4,5] | Edmund T. Rolls[9,10,11] | Ce-chen Sun[6] | Ling-hao Bu[1,2,3,4,5] | Jun-feng Lu[1,2,3,4,5] | Ching-po Lin[10] | Jian-feng Feng[9,10] | Ying Mao[1,2,3,4,5] | Liang-fu Zhou[1,2,3,4,5]

[1]Department of Neurosurgery, Huashan Hospital, Fudan University, Shanghai, China

[2]National Center for Neurological Disorders, Shanghai, China

[3]Shanghai Key Laboratory of Brain Function Restoration and Neural Regeneration, Shanghai, China

[4]Neurosurgical Institute of Fudan University, Shanghai, China

[5]Shanghai Clinical Medical Center of Neurosurgery, Shanghai, China

[6]Department of Biostatistics, School of Public Health, Fudan University, Shanghai, China

[7]National Clinical Research Centre for Aging and Medicine, Huashan Hospital, Fudan University, Shanghai, China

[8]Key Laboratory of Public Health Safety of Ministry of Education, Fudan University, Shanghai, China

[9]Department of Computer Science, University of Warwick, Coventry, UK

[10]Institute of Science and Technology for Brain-inspired Intelligence, Fudan University, Shanghai, China

[11]Oxford Centre for Computational Neuroscience, Oxford, UK

Correspondence
Jin-song Wu, Glioma Surgery Division, Neurologic Surgery Department, Huashan Hospital, Shanghai Medical College, Fudan University, No. 12 Middle Wulumuqi Rd., Shanghai, China.
Email: wujinsong@huashan.org.cn

Jian-feng Feng, Institute of Science and Technology for Brain-inspired Intelligence, Fudan University, Shanghai, China.
Email: jffeng@fudan.edu.cn

Funding information
National Natural Science Foundation of China, Grant/Award Number: 81271517; Shanghai Municipal Science and Technology Major Project, Grant/Award Number: No.2018SHZDZX01; Shanghai Shenkang Hospital Development Centre, Grant/Award Number: SHDC12018114

Abstract

The comprehension of spoken language is one of the most essential language functions in humans. However, the neurological underpinnings of auditory comprehension remain under debate. Here we used multi-modal neuroimaging analyses on a group of patients with low-grade gliomas to localize cortical regions and white matter tracts responsible for auditory language comprehension. Region-of-interests and voxel-level whole-brain analyses showed that cortical areas in the posterior temporal lobe are crucial for language comprehension. The fiber integrity assessed with diffusion tensor imaging of the arcuate fasciculus and the inferior longitudinal fasciculus was strongly correlated with both auditory comprehension and the grey matter volume of the inferior temporal and middle temporal gyri. Together, our findings provide direct evidence for an integrated network of auditory comprehension whereby the superior temporal gyrus and sulcus, the posterior parts of the middle and inferior temporal gyri serve as auditory comprehension cortex, and the arcuate fasciculus and the inferior

Abbreviations: AF/SLF, arcuate and superior longitudinal fasciculus; ILF, inferior longitudinal fasciculus; ITG, inferior temporal gyrus; LGGs, low-grade gliomas; MCA, middle cerebral artery; MTG, middle temporal gyrus; TMD, tumor maximum diameter; VLSM, voxel-based lesion symptom mapping.

Jie Zhang and Ye Yao contributed equally to the article.

longitudinal fasciculus subserve as crucial structural connectivity. These findings provide critical evidence on the neural underpinnings of language comprehension.

KEYWORDS
arcuate fasciculus, auditory comprehension, inferior longitudinal fasciculus, inferior temporal gyrus, middle temporal gyrus, superior longitudinal fasciculus

1 | INTRODUCTION

Auditory comprehension is a language processing supported by a neural basis that is often compromised after brain damage. Unable to understand auditory stimuli can affect all communication, for example, receiving instructions for prescription and treatment. Over the last century, the neural basis of auditory comprehension has been under intense investigation (DeWitt & Rauschecker, 2013; Hickok & Poeppel, 2007; Rauschecker & Scott, 2009). Seminal work by Lichteim (1885) based on post-mortem dissection suggested that Wernicke's area, which includes the posterior superior temporal gyrus (STG) and the superior temporal sulcus (STS), is the processing center for auditory language comprehension and that this region communicates with anterior speech execution regions, such as Broca's area, via projections to the frontal cortex through white matter fibers known as the arcuate fasciculus/superior longitudinal fasciculus (AF/SLF) (Margulies & Petrides, 2013; Martino et al., 2013). This proposed model of auditory processing is generally considered a milestone in the study of the brain's higher functions. However, emerging evidence from neuroimaging and lesion studies (Anderson et al., 1999; Bates et al., 2003; Dronkers et al., 2007; Miglioretti & Boatman, 2003) has suggested that deficits in auditory comprehension may not solely be caused by damage to the STG (Hickok & Poeppel, 2004). Furthermore, recent diffusion tensor imaging (DTI) and white matter dissection studies (Catani et al., 2005; Glasser & Rilling, 2008; Martino et al., 2013; Saur et al., 2008) identified several white matter fibers that may also play an essential role in language comprehension other than the AF/SLF.

Based on this line of evidence, it has been proposed that the neural basis of auditory processing can be divided into two functionally and anatomically distinct streams, following the two-stream hypothesis for vision (Goodale & Milner, 1992). Here, a dorsal motor-articulatory stream and a ventral conceptual-semantic stream are hypothesized to be responsible for auditory comprehension (Hickok & Poeppel, 2004, 2007; Rauschecker & Scott, 2009; Rauschecker & Tian, 2000). However, there is no consensus about which cortical regions are involved (Hickok & Poeppel, 2007; Rauschecker & Scott, 2009). One version of the auditory dual-stream model (Rauschecker & Scott, 2009; Rauschecker & Tian, 2000) holds that the STG/STS is essential for auditory comprehension. On the other hand, Hickok and Poeppel proposed that an extended temporal region, including the Middle Temporal Gyrus (MTG) and Inferior Temporal Gyrus (ITG), also plays a vital role (Hickok & Poeppel, 2007). Furthermore, white matter dissection and DTI studies showed that the ventral and dorsal streams, serving as connectional underpinnings of the language processing dual streams, could be further divided into several anatomically distinct fiber tracts with various cortical terminations (Fridriksson et al., 2018; Glasser & Rilling, 2008; Martino et al., 2013; Rilling, 2014; Rilling et al., 2008). Fridriksson et al. emphasized that short white matter tracts among the ITG, insula, and STG pole probably play a crucial role in sentence comprehension (Fridriksson et al., 2018), while others emphasize longer-range connections such as arcuate fasciculus and superior longitudinal fasciculus (Glasser & Rilling, 2008; Martino et al., 2013). Although these language-related fibers have been identified, their functional roles, for example, whether they are domain-general or specific, remain unclear (Dick & Tremblay, 2012; Friederici, 2015). Currently, the identification of cortical regions and white matter pathways involved in auditory comprehension remains controversial.

Here, we aimed to study the neural basis of auditory comprehension by examining the anatomical and functional correlations between auditory comprehension deficits and cortical damage, as well as white matter tract damage, in a cohort of low-grade gliomas (LGGs). We hypothesized that cortical areas and white matter tracts of both dorsal and ventral streams play an important role in auditory comprehension, and the damage of underlying white matter tracts could compromise auditory comprehension via the mediation from their cortical terminations. We used both the tumor structural indexes (e.g., maximum diameter) and VLSM to identify the influence of tumor characteristics and locations on auditory comprehension function. Regional and whole-brain voxel-wise analyses on gray matter volumes were investigated. Furthermore, the integrities of their correlated white matter fibers were analyzed using lesion load and fractional anisotropy, which made it possible to reveal the language network crucial for auditory comprehension. Finally, mediation analyses were done to find the causal relationship between functionally correlated cortices and white matter fibers. This study allows for a thorough investigation of how the damage to cortical regions and white matter tracts related to auditory comprehension performance and may provide evidence that the auditory comprehension process is mediated by not only ventral but also the dorsal streams.

2 | MATERIALS AND METHODS

2.1 | Participants

Patients were recruited from the Glioma Surgery Division in the Neurological Surgery Department at Huashan Hospital, Shanghai Medical College, Fudan University, Shanghai, China. From May 2011 to February 2015, 42 patients with grade II gliomas invading language-eloquent areas were included in this study.

TABLE 1 Demographic and behavioral data of patients ($n = 42$)

Demographic data	Mean (SD)	Min – Max
Age (years)	37.7 ± 10.4	22 – 61
Gender (males/females)	27/15	–
Education (years)	12.3 ± 4.3	0 – 20
Handedness (right/left)	42/0	–
Pathological diagnosis	–	
WHO grade	All subjects are WHO grade II patients	
Lesion volume (mm^3)	$6.5 \times 10^4 \pm 5.0 \times 10^4$	$8.0 \times 10^3 - 2.5 \times 10^5$
Behavioral data	**Mean (SD)**	***t*, *p***
KPS (%)	95.7 ± 5.0	5.0, 7.3×10^{-6}
MMSE (%)	89.7 ± 13.0	5.1, 7.1×10^{-6}
BNT (%)	73.4 ± 14.1	12.2, 2.9×10^{-15}
Aphasia battery of Chinese	–	
Aphasia quotient (%)	96.7 ± 3.8	5.5, 2.6×10^{-6}
Spontaneous speech (%)	98.1 ± 5.0	2.4, 0.023
Auditory comprehension (%)	96.3 ± 6.7	3.5, 0.0011
Repetition (%)	96.6 ± 6.2	3.4, 0.0015
Naming (%)	94.4 ± 6.5	5.5, 2.9×10^{-6}

Note: Lesion volume refers to tumor volume. The aphasia quotient was calculated based on the fluency, repetition, naming, and auditory comprehension scores. The percentage correct for each test is presented in the table. One-sample *T* test was conducted to compare the behavioral measurements of patients with the full scores (100%) of healthy controls. Abbreviations: BNT, Boston naming test; KPS, Karnofsky performance status; MMSE, mini mental state examination.

The inclusion criteria were as follows: native speakers of Chinese aged between 18 and 65 years old; righted-handedness assessed with the Edinburgh test. The tumor was located in the left frontal, temporal, parietal, or insular lobes with the pathological diagnosis of LGGs (WHO grade II). Patients with severe language deficits (AQ <50) or cognitive disorders (Mini-Mental State Examination [MMSE] <14) were excluded. All patients had no contradictions for MRI scanning. The mean age of the patients was 37.7 ± 10.4 years, and 27 of them were male. All patients showed no or mild language production deficits. The detailed demographic, clinical, and behavioral data are listed in Table 1. We also recruited 14 normal subjects (mean age 28.6 ± 8.6, 7 males) for DTI tractography analyses to create probabilistic maps for white matter tracts related to human language. Written informed consent was obtained from all participants, and the study was approved by the Huashan Hospital Institutional Review Board.

2.2 | Language and neuropsychological testing

All patients were tested for overall cognitive state by a neuropsychologist using the MMSE to exclude severe cognitive disorders (Pangman et al., 2000) (Figure 1).

To examine the essential region of the cerebral cortex leading to language comprehension impairment, in particular comprehension of spoken language, as previously defined as Wernicke's area (Margulies & Petrides, 2013), we applied the auditory comprehension subtest of the Aphasia Battery of Chinese (ABC), which is a Chinese standardized comprehensive language test adapted and modified from the Western Aphasia Battery (WAB). Patients' auditory comprehension performance was evaluated based on three subtests: yes/no questions, word recognition, and performance of sequential commands. We chose these tests based on the following rationales: First, LGG patients tend to present with mild cognitive deficits thus compared to other standard language tests, the auditory comprehension section of the WAB is more accurate and sensitive. Second, these tests were in accordance with the ones used by Bates et al. on a large cohort study of stroke patients and their auditory comprehension functions (Bates et al., 2003), which provided us an excellent opportunity to compare the two different brain lesion models. The local ethics committee checked and approved all tests. The same neuropsychologist assessed the cognitive and language functions of all patients.

2.3 | MRI data acquisition

MRI data were obtained in an iMRI-integrated neurosurgical suite (IMRIS) using a 3.0T scanner (MAGNETOM Verio 3.0T, Siemens AG). A fluid-attenuated inversion recovery (FLAIR) sequence was used for structural imaging (TR, 9000 ms; TE, 96 ms; TI, 2500 ms; flip angle, 150 degrees; slice thickness, 2 mm; FOV, $240 \times 240\ mm^2$; matrix size, 256×160). Diffusion-weighted images were acquired using a single-shot, spin-echo, echo planar imaging (EPI) sequence aligned with the anterior commissure-posterior commissure plane. The acquisition parameters were as follows: TR = 9700 ms; TE = 87 ms; matrix size = 122×122; slice number = 52; voxel size = $2 \times 2 \times 2\ mm^3$; *b*-value = 1000; directional = 30.

2.4 | Image preprocessing

Tumor lesions were delineated from the structural images by two senior neurosurgeons (J.Z. & J.S.W.) blind to the behavioral data. T2-FLAIR images were used for LGGs. The tumors were identified as the hyper-intense portion of the T2-FLAIR images according to Response Assessment in Neuro-Oncology (RANO) criteria (Wen et al., 2010). The drawing of tumor masks was initially generated using a semi-automated flood-fill algorithm (Agoston, 2005) available in MRICron software (http://www.mccauslandcenter.sc.edu/mricro/mricron/), according to the intensities of the different tissues. Then, the generated tumor masks were double-checked and manually refined by neurosurgeons (J.Z. & J.S.W.).

One obstacle neuroscientists face when analyzing brain tumors is the severe deformity of the brain by infiltrated tumors, which compromises the quality of the registration of the individual's brain into the standard space. To accomplish good registration in the present study, we applied a set of optimized cost function masking with the previously

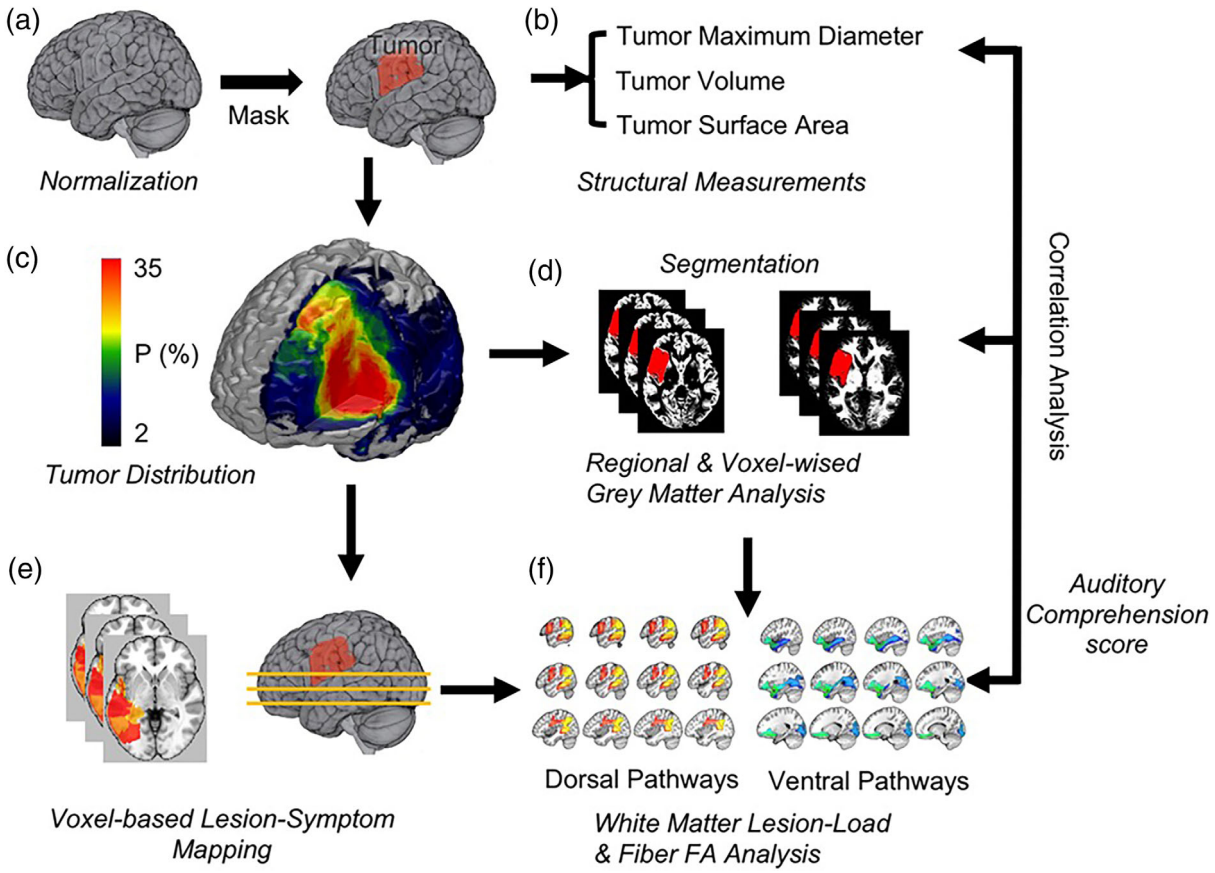

FIGURE 1 Research methodology flow (a) tumors were manually masked for all individuals. (b) Tumor structural measurements were extracted for all patients, including maximum tumor diameter, tumor volume, and tumor surface area. (c) The distribution of low-grade gliomas showed that the tumors were widely distributed throughout the left hemisphere. (d) Structural images were segmented into grey matter (left) and white matter (right). Grey matter volumes were calculated based on the AAL atlas for all brain regions. Voxel-wise grey matter intensity correlations were also performed. (e) Voxel-based lesion-symptom mapping was used to confirm the results from grey matter analysis. (f) The dorsal (left) and ventral (right) language pathways were individually traced in all subjects. Correlation analyses were performed to explore the relationship between tumor structural measurements, grey matter volumes of different brain regions, fasciculus characteristics, and auditory comprehension scores

drawn tumor lesion masks (Brett et al., 2001) to map the lesioned brain onto a standard Montreal Neurological Institute (MNI) template on a $1 \times 1 \times 1$ mm^3 scale (Tzourio-Mazoyer et al., 2002) and segmented grey matter for further analyses (Figure 1d). The lesion maps were spatially normalized into standard space using the previously obtained normalization parameters (Figure 1a). The resulting normalized images were visually inspected by one senior neurosurgeon (J.S.W.) and compared with the original lesions to ensure that the procedure was performed correctly. Figure 1c showed the overlap of lesions for 42 patients included and lesions were widely distributed in the frontal, temporal and parietal lobes. A detailed topography of tumor distribution is shown in Figure 2.

2.5 | Tumor characteristics analyses

To investigate the possible correlations between different tumor measures and language deficits, we calculated tumor structural measures (Safar & Shahabi, 2003) and Minkowski measures (Legland et al., 2011), including the tumor maximum diameter, volume, surface area, and mean curvature, for each patient (Figure 1b). Tumor maximum diameter was defined as the diameter of the bounding sphere that fully enclosed the tumor.

2.6 | Regional and whole-brain voxel-wise analyses on grey matter volume

Structural images were segmented into grey and white matter. The grey matter volume (GMV) within each of the 90 cerebral regions in the AAL atlas (Tzourio-Mazoyer et al., 2002) was calculated for each participant. Then the whole-brain voxel-wise analyses on GMV were performed using Voxel-based Morphometry (VBM) as well (Figure 1d).

2.7 | White matter fiber analyses

Using DTI and in vivo fiber tracking techniques, we delineated language-related white matter fibers to explore the relationships

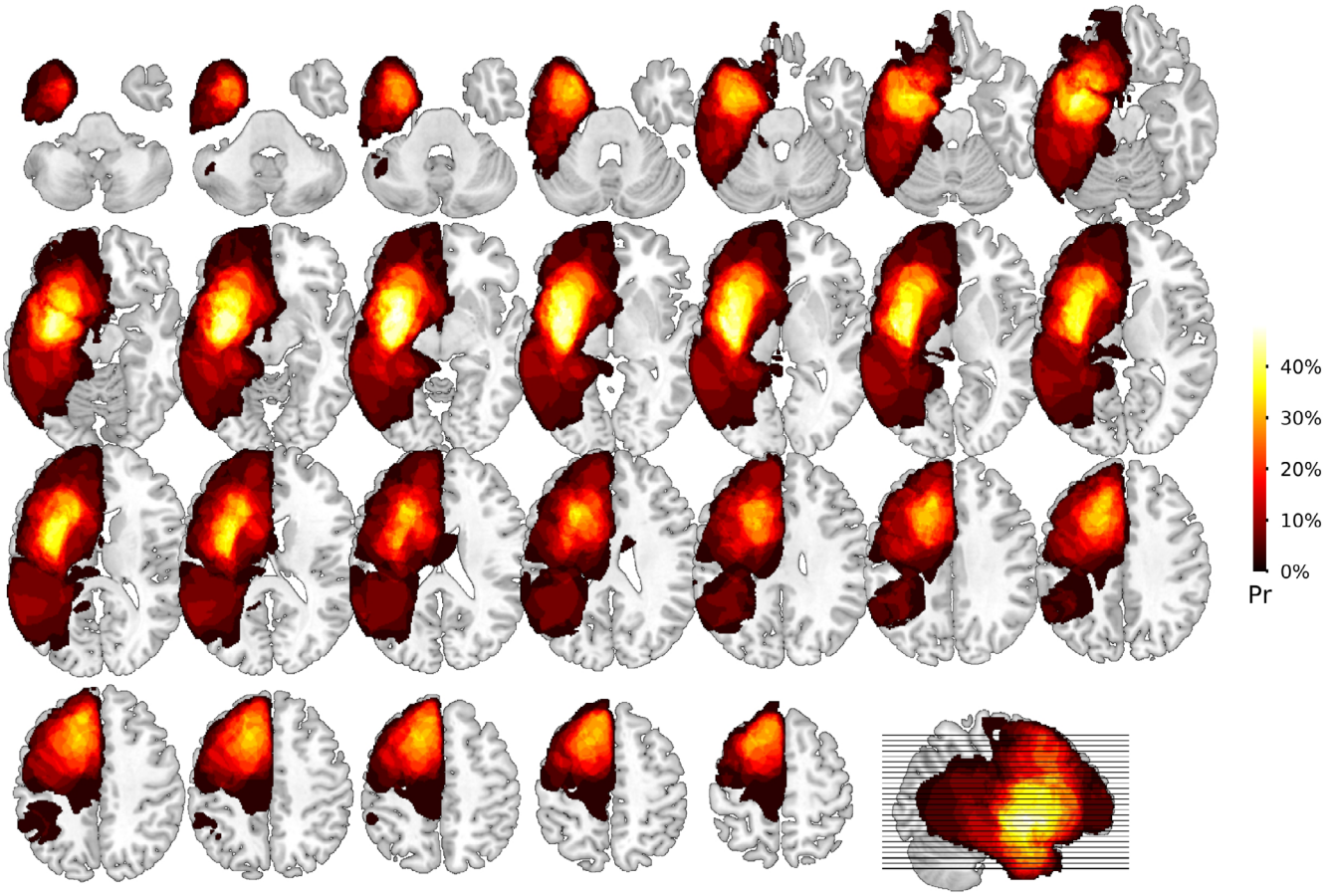

FIGURE 2 Topography of tumor distribution topography is shown using a heat map. The hotter the color is, the tumors of more patients are on the voxel

between white matter tracts and cortical regions (Figure 1f). We applied a multiple region of interest (ROI) approach to delineate fiber tracts of interest for language based on prior anatomical knowledge of the tracts. A detailed description of ROI methodology was provided by Wakana et al. (2007). For the dorsal pathways, we adapted the terms from the work of Catani et al. (2005), which included a direct long segment of the SLF (i.e., AF), as well as an anterior segment and a posterior segment. For the ventral pathways, the Inferior Fronto-Occipital Fasciculus (IFOF), the Inferior Longitudinal Fasciculus (ILF), and Uncinate Fasciculus (UF) were delineated according to the methods described by Wakana et al. (2007).

Then we assessed the fiber integrity of all tracts and their correlations with cortical volumes and the performance in auditory comprehension. Measurements of fiber integrities were based on two parameters: tumor lesion load and mean fractional anisotropy (FA). Both template-based analysis and the individual-based quantitative analysis of each fiber tract's fractional anisotropy (FA) were applied in this part. Since no fiber tract template is available for Asians, we calculated the probabilistic maps for white matter tracts related to human language based on 14 normal subjects using the same multiple region-of-interest (ROI) approach as the method in the latter individual analysis (Wakana et al., 2007).

In the 14 normal subjects, axonal projections were traced in both the anterograde and retrograde directions, according to the directions of the principal eigenvector in each voxel of the ROI. Tracking terminated when the FA value was lower than 0.15. The cortical connections of the tracts were inferred from the location and orientation of the average tract endpoints. Subsequently, we averaged the fiber tractography and created probabilistic templates for each tract (Figures S1 and S2). Then, the overlapping volumes of the tumor and the fiber templates we created above were calculated as the tumor lesion load for each patient. Furthermore, all fibers were tracked in each patient, and the mean FA of each tract was calculated in all patients using DSI Studio (Yeh et al., 2013) and the FMRIB software library (FSL) (Woolrich et al., 2009).

2.8 | Statistical analyses

We used multiple regressions to control for the effects of age and sex. We extracted the correlations between different measurements including tumor structural characteristics, grey matter volume of each brain region, tract measures, and auditory comprehension scores, with age and sex effects controlled. We showed the correlations between

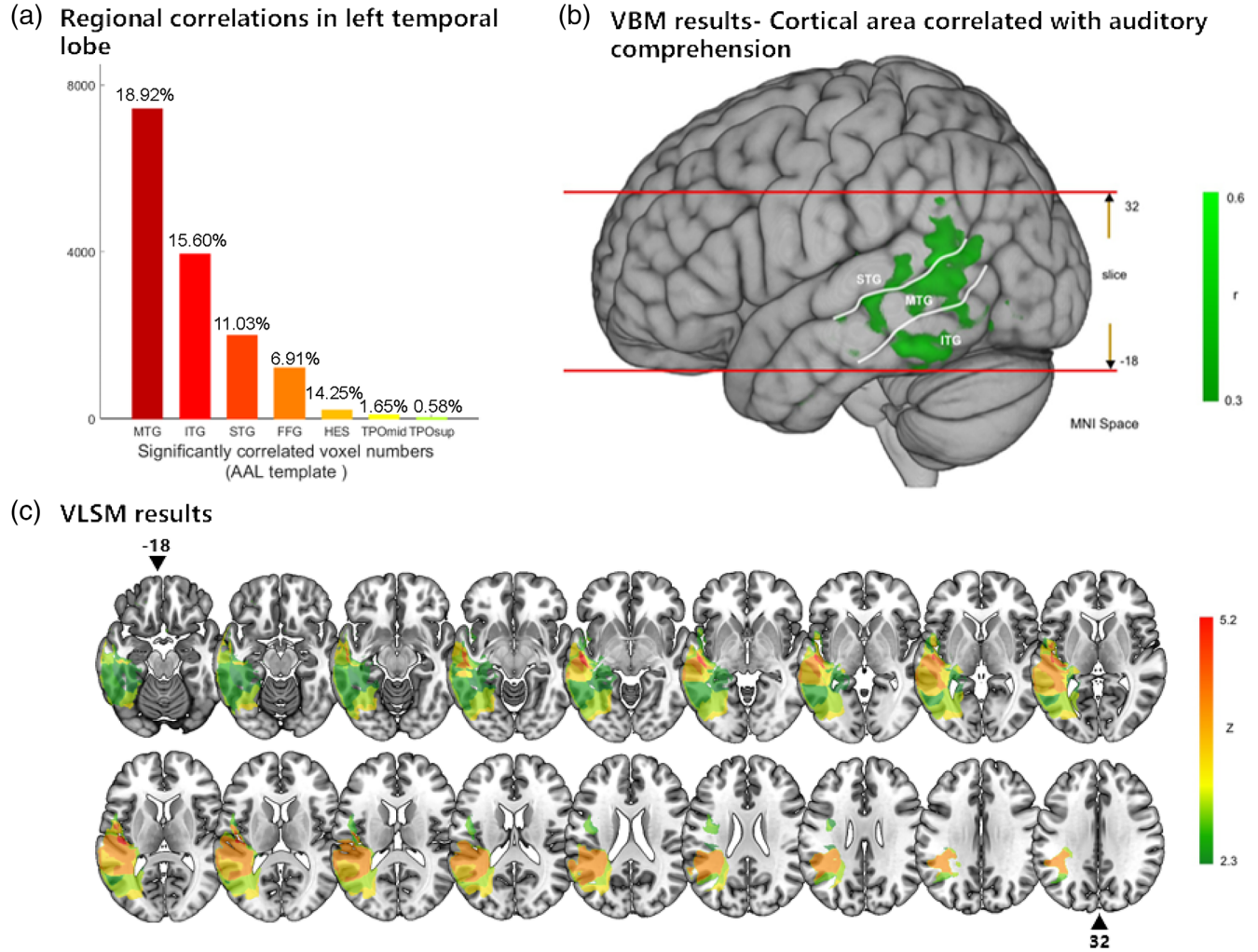

FIGURE 3 Voxel-wise correlations between grey matter volume (GMV) and auditory comprehension (a) voxel numbers significantly correlated with auditory comprehension scores were calculated within each temporal region. The percentage of voxel numbers within each temporal region was also given. (b) Voxel-wise correlations of grey matter volume and auditory comprehension were mapped on the cortical surface. The auditory comprehension correlated area was primarily located in the posterior temp lobe. (c) Voxel-based lesion symptom mapping (VLSM) results were consistent with the auditory comprehension correlation map. VLSM results also showed that lesions deep into the white matter of the posterior temporal lobe affected the auditory comprehension score

the grey matter volume of every voxel and auditory comprehension scores, with age and sex effects removed. We also performed Voxel-based Lesion Symptom Mapping (VLSM) to locate brain regions associated with auditory comprehension (Bates et al., 2003) (Figure 1). Specifically, patients were divided into two groups depending on whether normalized MRI images did or did not show damage to a specific voxel, with two-sample *t*-tests performed to compare their scores with covariable effects (age, sex, years of education) removed. This process was repeated for every voxel, yielding a set of t values. For multiple comparisons correction, we used cluster-level family-wise error correction via permutation testing, which randomly re-pairs the lesioned voxels with behavioral scores and re-runs the *t*-tests across all voxels. This test was repeated for 1000 times to determine how often high *t* values by chance. To locate brain regions, voxels were overlaid on the AAL atlas (Tzourio-Mazoyer et al., 2002). In addition, we used Cohen's *q* to quantify the effect size (i.e., the es) of the correlation coefficient (Rosenthal et al., 1994), and Bonferroni correction was carried out to correct for searching over 90 AAL atlas cerebral regions. All statistical analyses were performed using MATLAB software, version 2019b (MathWorks Inc.)

2.9 | Mediation analyses

To further investigate if the correlation between the white matter fibers and auditory comprehension is mediated by functionally related cortices, two-pathway mediation analyses were performed (Figure 6). In these analyses, we decomposed the total effects of white matter fiber damage on auditory comprehension into direct and indirect effects. According to our hypothesis that damage to structural connectivity could indirectly cause functional deficit via related cortical damage as a mediator, we conducted two separate

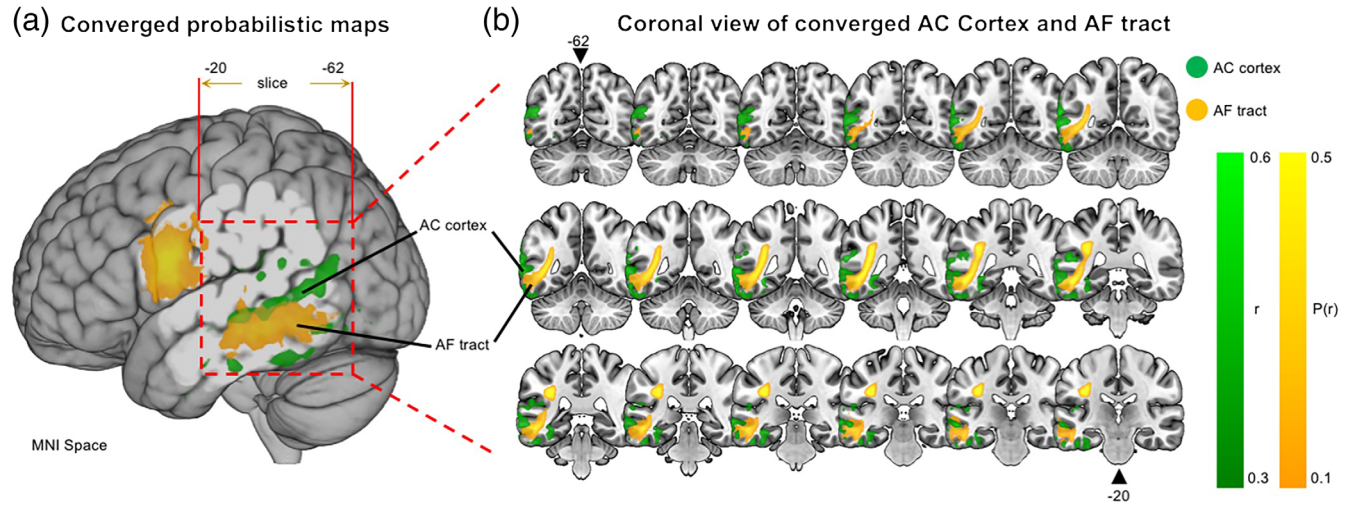

FIGURE 4 Converged probabilistic maps of auditory comprehension (AC) cortex and AF tract (a) all patients' arcuate fascicles were merged with the auditory comprehension correlation map with both thresholds above 10%. (b) The coronal view revealed that the cortical terminations of AF long segment were spatially connected to the auditory comprehension correlated area

mediation analyses to investigate the mediation effects of MTG and ITG on the link between white matter fiber damage and auditory comprehension, respectively. To assess the indirect effects, we first calculated the relation between white matter tract damage and MTG or ITG damage when other mediators were controlled. Then we calculated the impact of MTG or ITG damage on comprehension when other mediators and white matter damage were controlled. A bootstrapping approach was applied to testify the hypothesis, and the null hypothesis (no indirect effect present) was rejected if the *p*-value was not smaller than .05.

3 | RESULTS

3.1 | Tumor characteristics analyses results

We manually delineated and extracted the anatomical characteristics of tumors and compared them with patients' behavioral data to examine the effect of tumorigenesis on language functions. Among all the tumor structural measures and Minkowski results, we found the maximum diameter of the tumor to be significantly correlated ($r = -0.51$, $p = .0016$, es $= -0.56$) with auditory language comprehension. In contrast, no significant correlation was found between the patient's age and auditory language comprehension. Tumor volume was also a predictor other than the maximum diameter ($r = -0.46$, $p = .0048$, es $= -0.56$) (Figure S3a).

3.2 | Regional and whole-brain voxel-wise analyses

After extracting the correlations between the GMVs of 90 cerebral regions in the AAL atlas (Tzourio-Mazoyer et al., 2002) and auditory comprehension scores, with age, sex, and total intracranial volume effects removed, we found that the grey matter in the posterior temporal lobe had a fairly significant correlation with auditory comprehension, especially in MTG and ITG, with $r = 0.529$, $p = 9.1 \times 10^{-4}$ and $r = 0.541$, $p = 6.6 \times 10^{-4}$, respectively, Bonferroni corrected. Besides, the grey matter of STG also showed a positive correlation ($r = 0.396$, $p = .017$), which could pass the permutation test correction. Moreover, significant negative correlations were also found between the grey matter of the ITG and MTG and the maximum diameter of the tumor ($r = -0.485$, $p = .0027$, es $= -0.530$ and $r = -0.422$, $p = .0103$, es $= -0.450$, respectively) (Figure S3b,c), indicating the tumor-induced grey matter volume decrease within MTG and ITG was the underlying cause of auditory comprehension impairment.

The results of the whole-brain voxel-wise correlation analyses between grey matter and auditory comprehension were projected onto the cortical surface of the brain to identify the areas involved (Figure 3a,b). A large cluster in the posterior temporal lobe was found, verifying the above findings in a data-driven, atlas-free approach. As for the number of voxels significantly correlated with auditory comprehension scores, MTG, ITG and STG ranked among the top three, with 18.8%, 15.3%, and 10.5%, respectively. We conducted exact (significance) test and found that the results of VLSM and VBM are highly similar ($z = 3.818$, $p = 6.7 \times 10^{-5}$) (Table S1). VLSM analysis supported the result that auditory comprehension was affected mainly by lesions in the posterior part of the ITG and MTG (Figure 3c).

3.3 | White matter fiber analyses results

The results of VLSM above have revealed that auditory comprehension can be affected by not only lesions in the posterior temporal region but also lesions in the underlying white matter. For the dorsal

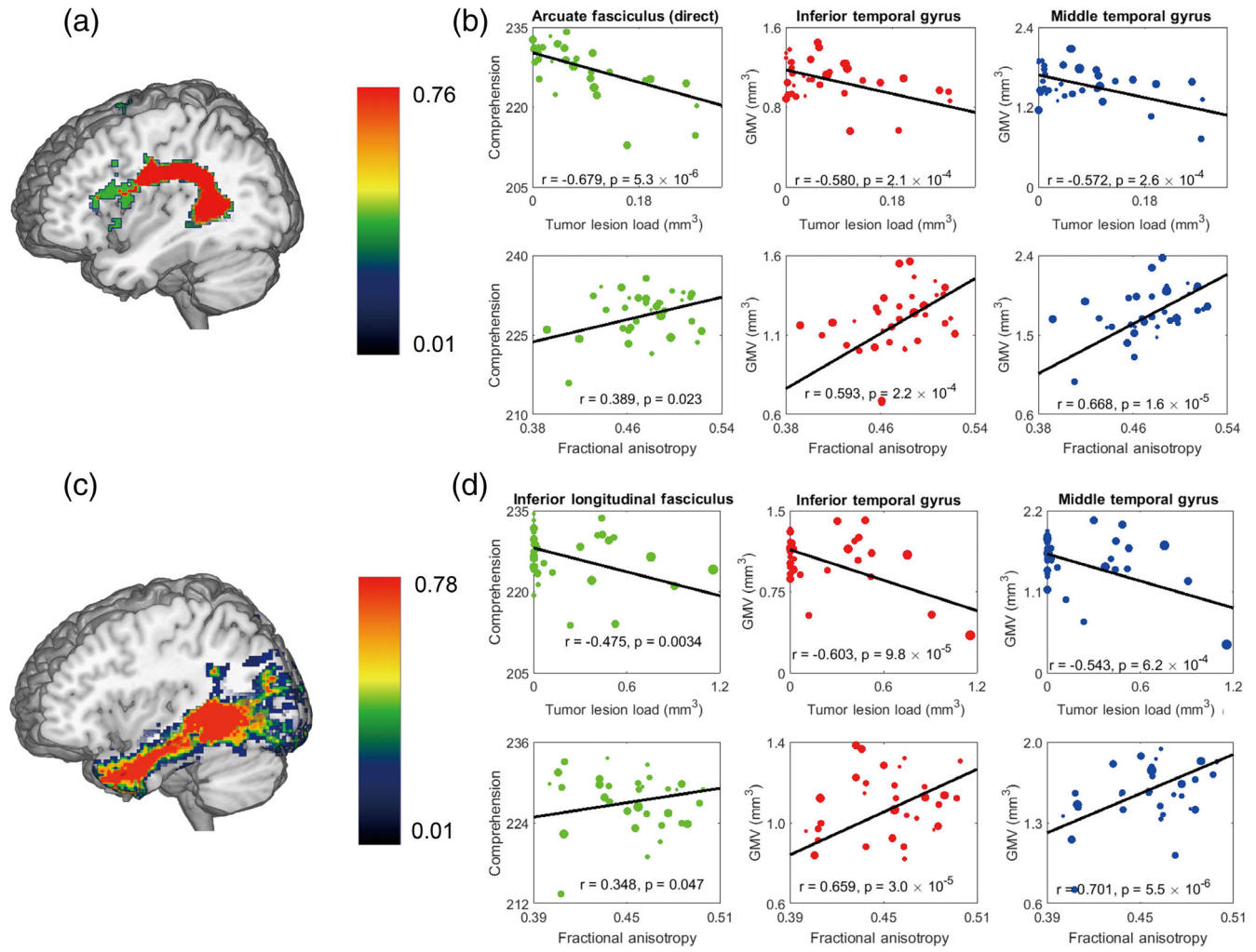

FIGURE 5 Multiple regression analyses of tumor lesion load of the language ventral pathway. (a) the probabilistic map was generated for arcuate fasciculus (AF). (b) Grey matter volumes of the inferior temporal gyrus (ITG) and middle temporal gyrus (MTG) were negatively correlated with AF lesion load (upper row) and positively correlated with mean FA (lower row). (c) Probabilistic map generated for ILF. (d) Auditory comprehension was negatively correlated with ILF lesion load (upper row) and positively correlated to mean FA (lower row). The size of the dot represents the tumor maximal diameter (the diameter of the bounding sphere that fully enclosed the tumor)

stream, as demonstrated in Figure 4, a large overlap was found between the cortical terminations of AF and the regions related to auditory comprehension in GMV analyses. Moreover, after controlling for age and sex, multiple regression analyses showed that auditory comprehension performance was negatively associated ($r = -0.679$, $p = 5.3 \times 10^{-6}$, es $= -0.827$, Bonferroni corrected) with the AF lesion load and positively correlated ($r = 0.389$, $p = .023$, es $= 0.411$, Bonferroni corrected) with the mean FA of the AF (Figure 5a,b). Importantly, the volumes of the ITG and MTG were negatively correlated with the AF lesion load (see details in Table 2) ($r = -0.580$, $p = 2.1 \times 10^{-4}$, es $= -0.663$; $r = -0.572$, $p = 2.6 \times 10^{-4}$, es $= -0.651$, Bonferroni corrected), and positively correlated with mean FA ($r = 0.593$, $p = 2.2 \times 10^{-4}$, es $= 0.683$; $r = 0.668$, $p = 1.6 \times 10^{-5}$, es $= 0.807$, Bonferroni corrected). However, neither the anterior nor the posterior segment of the SLF showed a significant correlation with auditory comprehension performance (Figure S4c,d).

ILF, one of the main pathways of the ventral stream, went underneath the corresponding cortical regions found in GMV analyses (Figure S5). A quantitative analysis revealed a significant correlation between auditory comprehension and the ILF integrity (lesion load: $r = -0.475$, $p = .0034$, es $= -0.517$; mean FA: $r = 0.348$, $p = .047$, es $= 0.363$, Bonferroni corrected) (Figure 5c,d). Furthermore, as the tumor lesion load of the ILF increased, the volumes of the ITG and MTG decreased significantly ($r = -0.603$, $p = 9.8 \times 10^{-5}$, es $= -0.700$, $r = -0.543$, $p = 6.2 \times 10^{-4}$, es $= -0.608$, respectively, Bonferroni corrected), as did the mean FA of the ILF ($r = 0.659$, $p = 3.0 \times 10^{-5}$, es $= 0.791$, $r = -0.701$, $p = 5.5 \times 10^{-6}$, es $= -0.869$, Bonferroni corrected) (Figure 5d). The measures for the IFOF and UF were not correlated with auditory comprehension performance (Figure S4e–h).

As shown in Figure 6, the mediation analyses revealed no significant direct effect of AF damage on auditory comprehension scores.

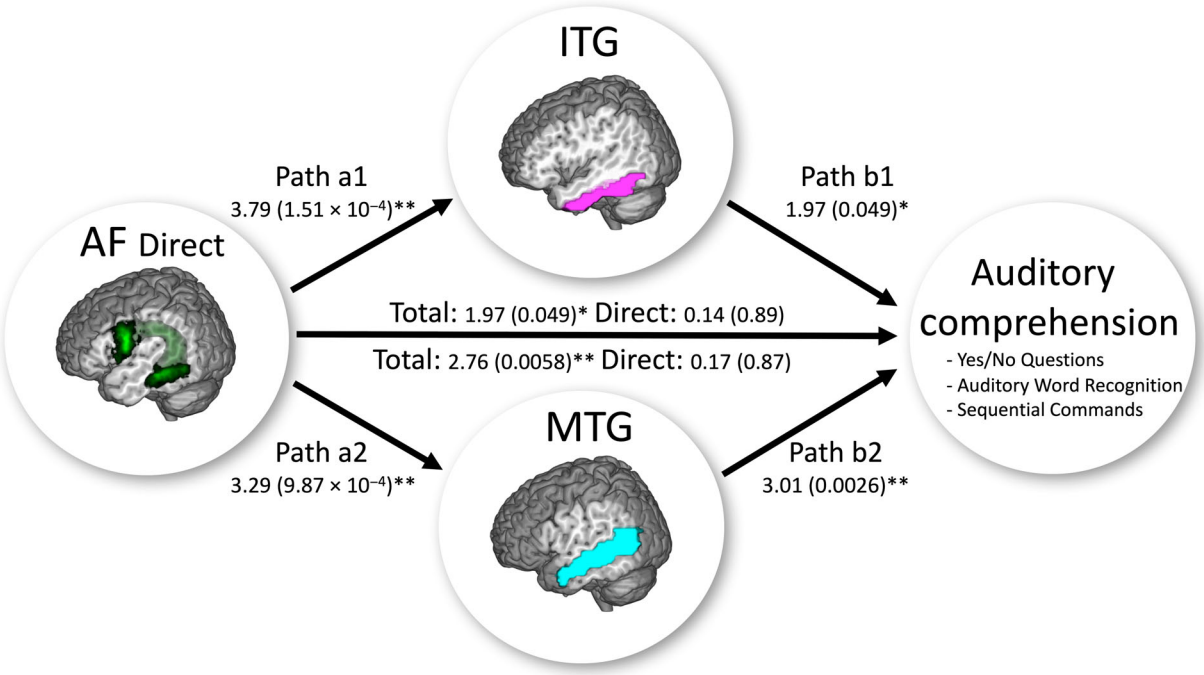

FIGURE 6 Mediation model and hypotheses. No significant direct effect of AF damage on auditory comprehension scores was observed. However, the two indirect effects through the mediators-damage in MTG or ITG cortices-were significant

However, there were substantial indirect effects from the damage of MTG/ITG. The proportion of indirect effects from the damage of MTG and ITG to the total effect is 93.84% and 92.39%, respectively. In other words, lesioned AF was associated with impairments involving MTG and ITG cortices, which would lead to lower auditory comprehension scores. Thus, the total effects of AF damage on auditory comprehension scores were mainly because of indirect effects via posterior temporal cortical impairment rather than the direct impact of white matter tract damage.

4 | DISCUSSION

Using lesion-based, multi-regression analysis on structural and diffusion MRI data in a group of glioma patients, we investigated the critical cortical areas and structural connectivity underlying auditory comprehension and their causal relationships. First, we used ROI-based and whole-brain voxel-wise analyses and identified that the cortical regions in the posterior temporal lobe, including MTG and ITG, were most strongly correlated with auditory language comprehension. To investigate the structural connectivity underlying auditory comprehension, we evaluated the fiber integrities of language-related fiber tracts and found that the fiber integrities of the ILF and the AF were correlated with auditory comprehension and also with the grey matter volumes of ITG/MTG. Furthermore, by merging language-related fiber tracts with a voxel-wise correlation map of auditory comprehension, we showed that the spatial connections between the AF terminations and the posterior temporal cortices correlated with auditory comprehension. The causal relations of cortical regions and their structural connectivity were investigated by mediation analyses, which confirmed our hypothesis that the damage of AF could compromise auditory comprehension via the mediation from cortical areas located in posterior temporal regions. These lines of evidence indicate that the posterior MTG, ITG, and the dorsal and the ventral pathway are important in auditory comprehension; and provide explanations that gliomas can cause functional deficit through the white matter pathway as long as they are connected to the responsible functional cortices.

According to the classical Wernicke-Lichtheim model (Lichteim, 1885), impaired auditory comprehension with intact fluency is associated with lesions in Wernicke's area. However, the exact definition of Wernicke's area has been widely disputed (Binder, 2015). A widely accepted anatomical definition of this area includes only posterior STG (pSTG) and supramarginal gyrus. In contrast, Bogen and Bogen (1976) defined Wernicke's area from its functional role as "the area where a lesion will cause language comprehension deficit," including a broader range of posterior temporal lobe and inferior parietal lobule.

The current study confirmed the STG with auditory comprehension, with peak voxels mainly located in the pSTG, Recent studies based on functional neuroimaging (Price, 2012; Wilson et al., 2018) and direct electrocorticography (Yi et al., 2019) have demonstrated that STG, as well as the posterior dorsal bank of STS, is the critical region to store and activate phonological forms in speech production (so-called phonological representation). Lesion-deficit correlation studies have shown that focal damage within this area caused phonological paraphasia (Gorno-Tempini et al., 2008; Rohrer et al., 2010). Another evidence that cortical electrical stimulation in this area could

TABLE 2 Correlation between grey matter volume/white matter tract integrity and auditory comprehension

Region	Mean volume (mm^3)	No. of patients with lesion in the ROI	Grey matter volume-behavior correlation
ITG	$1.1 \times 10^4 \pm 3.1 \times 10^3$	13 subjects	$r = 0.54, p = 6.6 \times 10^{-4}$[b]
MTG	$1.7 \times 10^4 \pm 4.6 \times 10^3$	15 subjects	$r = 0.53, p = 9.1 \times 10^{-4}$[b]
STG	$7.7 \times 10^3 \pm 2.0 \times 10^3$	21 subjects	$r = 0.39, p = .019$[a]
Tract integrity (measured by lesion load and mean FA)			
Tract	**Mean volume (mm^3)**	**No. of patients with lesion**	**Lesion load-behavior correlation**	**Mean FA-behavior correlation**
AF_L	$1.2 \times 10^4 \pm 5.6 \times 10^3$	16 subjects	$r = -0.68, p = 5.3 \times 10^{-6}$[b]	$r = 0.39, p = .023$[a]
AF_A	$5.6 \times 10^3 \pm 3.9 \times 10^3$	4 subjects	$r = -0.43, p = .0089$[a]	$r = 0.043, p = .83$
AF_P	$1.1 \times 10^4 \pm 5.3 \times 10^3$	4 subjects	$r = -0.57, p = 3.1 \times 10^{-4}$[a]	$r = 0.26, p = .16$
ILF	$2.1 \times 10^4 \pm 7.1 \times 10^3$	18 subjects	$r = -0.48, p = .0034$[a]	$r = 0.35, p = .047$[a]
UF	$9.3 \times 10^3 \pm 4.4 \times 10^3$	17 subjects	$r = -0.12, p = .47$	$r = 0.15, p = .42$
IFOF	$1.9 \times 10^4 \pm 6.9 \times 10^3$	23 subjects	$r = -0.28, p = .098$	$r = 0.29, p = .10$

Note: The correlation analyses were conducted in all patients.
Abbreviations: AF_A, anterior segment of arcuate fasciculus; AF_L, long segment of arcuate fasciculus; AF_P, posterior segment of arcuate fasciculus; IFOF, inferior fronto-occipital fasciculus; ILF, inferior longitudinal fasciculus; ITG, inferior temporal gyrus; MTG, middle temporal gyrus; STG, superior temporal gyrus; UF, uncinate fasciculus.
[a]Significantly correlated.
[b]Most significantly correlated with auditory comprehension.

elicit phonological error without disruption of comprehension further supported the above statement (Corina et al., 2010; Sarubbo et al., 2019).

Our findings of the strong correlation between posterior MTG (pMTG) and auditory comprehension were consistent with those seen in functional neuroimaging (Price, 2012) and lesion-symptom analysis (Bates et al., 2003; Bonilha et al., 2017; Fridriksson et al., 2018). The pMTG was believed to be the hub of language comprehension (Binder, 2017). Recently, Matchin and Hickok (2019) postulated a hierarchical lexical-syntactic function to pMTG, necessary for auditory comprehension. Specifically, the role of pMTG during auditory comprehension was to analyze the phonological representations and then communicate with the conceptual networks to form conceptual-semantic representations.

Our results indicated that the ITG played a critical role in the auditory comprehension process. Although ITG has long been regarded as a part of the ventral stream of visual processing (Goodale & Milner, 1992; Mishkin et al., 1983), serving in object (Gaillard et al., 2006; Rolls, 2012; Turkeltaub et al., 2003) and word recognition (Nobre et al., 1994), its role in semantic processing has only been under investigation recently (Bonilha et al., 2017; Trimmel et al., 2018). Bonilha et al. (2017) found a small area in posterior ITG, which was in close vicinity of our results, had a strong correlation to spoken word comprehension when controlling for amodal semantic processing. A meta-analysis of 120 function neuroimaging studies revealed that activation of ITG was found during semantic processing tasks (Binder et al., 2009). Taken together, our findings support that pMTG serve as a comprehension hub by linking the initial phonological processing in STG and the later semantic processing in ITG, enabling auditory stimuli turn into phonological and semantic representations.

The auditory comprehension process is an integrated yet widely distributed system connected by white matter tracts (Friederici, 2015; Hickok & Poeppel, 2007). While cortices related to auditory comprehension have been identified, their subcortical underpinnings and functional roles remain unclear (Friederici, 2015). Our DTI analyses based on both lesion load and FA value confirmed the strong correlations between auditory comprehension scores and AF, as well as ILF, indicating that auditory comprehension recruits a network composed of both dorsal and ventral streams. Consistent with previous research suggesting that clinical tasks of aphasia involve many different processes that rely on two streams (Fridriksson et al., 2018).

Anatomically, the ILF has been identified as a ventral associative bundle that connects the occipital lobe and the temporal pole with short fibers, which terminates in the ITG, MTG, hippocampus, and amygdala (Catani et al., 2003; Latini et al., 2017; Tusa & Ungerleider, 1985). Based on its anatomical terminations, we believe that ILF plays an important role in semantic processing. Evidence from patients with semantic dementia (Acosta-Cabronero et al., 2011; Agosta et al., 2010), a semantic variant of primary progressive aphasia (Agosta et al., 2013), and stroke-induced aphasia (Ivanova et al., 2016) showed the potential association between ILF and semantic processing. It was recently proposed by Duffau (2015) that ILF played a role in a semantic ventral stream based on evidence from subcortical electrical stimulations. The role of ventral stream may be especially crucial in tonal languages such as Mandarin Chinese. In Mandarin Chinese, the extensive use of homophones makes the sound-meaning mapping processing more complex, thus placing a higher demand on phonological and further semantic processing to identify words in tonal language (Ge et al., 2015).

Our findings also showed that the auditory comprehension process depends on the dorsal language fiber tracts, especially the

long segment of the SLF (i.e., AF). Our fiber tracking results showed that the temporal lobe projections of the AF mainly terminate in the posterior part of the ITG and MTG, where the auditory comprehension cortex is located (Figure 4). One comparative DTI study (Rilling et al., 2008) showed that the cortical terminations of the AF in humans differed from nonhuman primates. Specifically, much stronger projections to the posterior temporal cortex were observed in ITG and MTG. Recent DTI and fiber dissection studies also showed that AF primarily connects the MTG and ITG with the precentral gyrus and posterior portion of the inferior and middle frontal gyri (Catani & Thiebaut de Schotten, 2008; Glasser & Rilling, 2008; Martino et al., 2013). Wilson et al. (2011) found the reduced FA in left AF was strongly associated with syntactic comprehension in a sentence-to-picture matching task. Zaccarella et al. (2017) further proposed that AF, which connected the Broca's area and posterior temporal lobe, was the core white matter tract in syntactic processing. Thus, the correlation between AF and auditory comprehension in the current study may be attributed to impaired syntactic processing, especially in subtests of Yes/No questions and sequential commands. Our mediation analysis results showed that the AF indirectly affected auditory comprehension through the ITG/MTG (Figure 6). This result should be interpreted with caution as it was derived from cross-sectional data (Hill, 1965; Jose, 2016). However, we believe sufficient rationale for posited mediation process exists. Previous studies have supported the neural basis of AF direct white matter pathway effects on ITG and MTG. AF primarily connects the MTG and ITG with the precentral gyrus and posterior portion of the inferior and middle frontal gyri (Catani & Thiebaut de Schotten, 2008; Glasser & Rilling, 2008; Martino et al., 2013). Moreover, axonal degeneration explains why AF damage leads to reduced functioning in the MTG and ITG. Axonal degeneration may affect the axon distal to the focal damage, which causes a cascade of events (Crowe et al., 1997). Since AF is anatomically connected to MTG and ITG, the retrograde degeneration of the AF would likely lead to neuronal atrophy in the ITG/MTG, resulting in defective auditory comprehension.

In this study, high-resolution FLAIR was used for VBM analysis to assess grey matter (GM) volume, which is indeed different from most VBM studies based on T1 images. We employed FLAIR-VBM based on the following considerations. First, conventional VBM mainly used in healthy subjects or patients without severe deformity. In this study, the severe deformity of the brain by infiltrated LGGs greatly compromises the quality of the registration of the individual's brain into the standard space. In this case, T1 images often cannot distinguish between tumors and cortical signals, while FLAIR can present differences in signal intensity between tumor and normal tissue. Second, the advantage of FLAIR is presenting differences in signal intensity between dura and cortical gray matter. It has also been shown that standard segmentation based only on T1 images overestimates gray matter volume by wrongly assigning vessels and dura to this compartment and that the combination of T1 and FLAIR images results in better segmentation (Diaz-de-Grenu et al., 2011; Lindig et al., 2018). However, out of considerations for patient cooperation, scan times, and the economy cost, we choose multi-layer FLAIR images for preoperative navigation and data analysis. Meanwhile, two neurosurgeons (J.Z. & J.S.W.) visually inspect the normalized, modulated images case by case, to ensure the reliability and accuracy of image data.

LGGs are a group of tumors that migrate along the white matter tracts with a linear increase of the mean diameter around 4 mm per year (Duffau, 2013). The increasing application of object cognitive assessments on LGG patients has changed the old view that LGGs rarely cause neurological deficits. However, the exact mechanism of LGG-induced brain function impairments, especially language deficits, remains unknown. The current study focused on the auditory comprehension ability in LGG patients, revealing that the impairment of the posterior temporal lobe and white matter tracts (e.g., AF and ILF) was associated with the deficits. A further mediation analysis suggested that the axonal degeneration of fiber tracts (e.g., AF) may lead to atrophy in cortical areas, which in turn causes neurological deficits. This mechanism could answer the phenomenon that patients with tumors in the frontal lobe, especially in the subcortical white matter, also showed auditory comprehension deficits. Thus, LGGs could directly cause neurological deficits by invading the critical brain structures or indirectly, through the infiltration of white matter tracts, leading to retrograde degeneration of grey matter.

4.1 | Limitations

Several limitations of this study should be noted. First, based on the infiltrative nature of LGGs, some cortical areas might still have residual function, despite the structural abnormalities observed with imaging. We could not take into account these infiltrated cortices during our VBM analysis and cannot determine the direct impact of tumors on some of the frontal regions, which may also affect VLSM results and lead to bias. However, since the lesion distribution in LGG patients is comparatively broader than in other brain disorders, the bias effects are inevitable but not large enough to be fatal (Mah et al., 2014). Second, several subprocesses, such as pitch and tone processing, phonologic and syntactic interpretation, may also be involved in the auditory comprehension process alongside the sound-meaning mapping process. Further studies of these subprocesses are needed to develop a more detailed model of auditory comprehension processing. Third, we applied mediation analysis to examine causal relationships between different brain areas and comprehension scores, the results should be interpreted with caution since no temporal information was available (Hill, 1965; Jose, 2016). An alternative approach is to use high temporal resolution methods such as electrocorticography (ECoG) rather than mediation analysis. In fact, in our recent study (Zhu et al., 2022), we applied high-density (ECoG) to measure the temporal properties of syntactic processing. However, this approach can only be applied on the cortical surface, limiting its usage in deep structures such as white matter tracts.

5 | CONCLUSIONS

In conclusion, our results show that other than the classic Wernicke's area, the posterior temporal region, including the MTG and ITG, also significantly contribute to auditory comprehension. The ILF and the AF may serve as structural connectivity for auditory comprehension, and gliomas can impair auditory comprehension indirectly by infiltration of the AF and ILF, which causes retrograde degeneration of grey matter in the ITG and MTG. Our results suggest that auditory comprehension is a complex, integrated process involving the participation of both the dorsal and ventral language pathways.

AUTHOR CONTRIBUTIONS

Jin-song Wu and Jian-feng Feng designed the experiments. Jie Zhang and Jun-feng Lu recruited patients and healthy controls and collected the MRI data samples. Ye Yao, Jie Zhang, and Ling-hao Bu preprocessed the structural MRI data and analyzed related statistics. Ye Yao, Jie Zhang, and Ching-po Lin processed the DTI data and analyzed related statistics. Jie Zhang, Ye Yao, Jin-song Wu, Jian-feng Feng, Ce-chen Sun, and Edmund T. Rolls wrote the manuscript. Ying Mao, Edmund T. Rolls & Liang-fu Zhou supervised this study and revised the manuscript. All authors discussed the results and commented on the manuscript.

ACKNOWLEDGMENTS

This study was funded by the National Natural Science Foundation of China (81271517), Shanghai Shenkang Hospital Development Centre (SHDC12018114), Shanghai Municipal Science and Technology Major Project (No. 2018SHZDZX01), and the National Centre for Mathematics and Interdisciplinary Sciences (NCMIS) of the Chinese Academy of Sciences, and ZJLab. We would also like to thank Zhong Yang for the help with MRI data acquisition and Yan Zhou for behavioral data collection.

CONFLICT OF INTERESTS

The authors declare no conflict of interests.

DATA AVAILABILITY STATEMENT

The data that support the findings of this study are available on request from the corresponding author. The data are not publicly available due to privacy or ethical restrictions.

ORCID

Jie Zhang https://orcid.org/0000-0002-6805-8474
Ye Yao https://orcid.org/0000-0002-0878-8942
Jin-song Wu https://orcid.org/0000-0001-7854-9798
Edmund T. Rolls https://orcid.org/0000-0003-3025-1292
Ce-chen Sun https://orcid.org/0000-0001-6074-8801

REFERENCES

Acosta-Cabronero, J., Patterson, K., Fryer, T. D., Hodges, J. R., Pengas, G., Williams, G. B., & Nestor, P. J. (2011). Atrophy, hypometabolism and white matter abnormalities in semantic dementia tell a coherent story. *Brain*, *134*, 2025–2035. https://doi.org/10.1093/brain/awr119

Agosta, F., Galantucci, S., Canu, E., Cappa, S. F., Magnani, G., Franceschi, M., Falini, A., Comi, G., & Filippi, M. (2013). Disruption of structural connectivity along the dorsal and ventral language pathways in patients with nonfluent and semantic variant primary progressive aphasia: A DT MRI study and a literature review. *Brain and Language*, *127*, 157–166. https://doi.org/10.1016/j.bandl.2013.06.003

Agosta, F., Henry, R. G., Migliaccio, R., Neuhaus, J., Miller, B. L., Dronkers, N. F., Brambati, S. M., Filippi, M., Ogar, J. M., Wilson, S. M., & Gorno-Tempini, M. L. (2010). Language networks in semantic dementia. *Brain*, *133*, 286–299. https://doi.org/10.1093/brain/awp233

Agoston, M. K. (2005). *Computer graphics and geometric modelling: Implementation & algorithms*. Springer.

Anderson, J. M., Gilmore, R., Roper, S., Crosson, B., Bauer, R. M., Nadeau, S., Beversdorf, D. Q., Cibula, J., Rogish, M., III, Kortencamp, S., Hughes, J. D., Gonzalez Rothi, L. J., & Heilman, K. M. (1999). Conduction aphasia and the arcuate fasciculus: A reexamination of the Wernicke-Geschwind model. *Brain and Language*, *70*, 1–12. https://doi.org/10.1006/brln.1999.2135

Bates, E., Wilson, S. M., Saygin, A. P., Dick, F., Sereno, M. I., Knight, R. T., & Dronkers, N. F. (2003). Voxel-based lesion-symptom mapping. *Nature Neuroscience*, *6*, 448–450. https://doi.org/10.1038/nn1050

Binder, J. R. (2015). The Wernicke area: Modern evidence and a reinterpretation. *Neurology*, *85*, 2170–2175. https://doi.org/10.1212/wnl.0000000000002219

Binder, J. R. (2017). Current controversies on Wernicke's area and its role in language. *Current Neurology and Neuroscience Reports*, *17*, 58. https://doi.org/10.1007/s11910-017-0764-8

Binder, J. R., Desai, R. H., Graves, W. W., & Conant, L. L. (2009). Where is the semantic system? A critical review and meta-analysis of 120 functional neuroimaging studies. *Cerebral Cortex (New York, N.Y.: 1991)*, *19*, 2767–2796. https://doi.org/10.1093/cercor/bhp055

Bogen, J. E., & Bogen, G. M. (1976). Wernicke's region—Where is it. *Annals of the New York Academy of Sciences*, *280*, 834–843. https://doi.org/10.1111/j.1749-6632.1976.tb25546.x

Bonilha, L., Hillis, A. E., Hickok, G., den Ouden, D. B., Rorden, C., & Fridriksson, J. (2017). Temporal lobe networks supporting the comprehension of spoken words. *Brain*, *140*, 2370–2380. https://doi.org/10.1093/brain/awx169

Brett, M., Leff, A. P., Rorden, C., & Ashburner, J. (2001). Spatial normalization of brain images with focal lesions using cost function masking. *NeuroImage*, *14*, 486–500. https://doi.org/10.1006/nimg.2001.0845

Catani, M., Jones, D. K., Donato, R., & Ffytche, D. H. (2003). Occipito-temporal connections in the human brain. *Brain*, *126*, 2093–2107. https://doi.org/10.1093/brain/awg203

Catani, M., Jones, D. K. & Fytche, D. H. (2005). Perisylvian language networks of the human brain. *Annals of Neurology*, *57*, 8–16. https://doi.org/10.1002/ana.20319

Catani, M., & Thiebaut de Schotten, M. (2008). A diffusion tensor imaging tractography atlas for virtual in vivo dissections. *Cortex*, *44*, 1105–1132. https://doi.org/10.1016/j.cortex.2008.05.004

Corina, D. P., Loudermilk, B. C., Detwiler, L., Martin, R. F., Brinkley, J. F., & Ojemann, G. (2010). Analysis of naming errors during cortical stimulation mapping: Implications for models of language representation. *Brain and Language*, *115*, 101–112. https://doi.org/10.1016/j.bandl.2010.04.001

Crowe, M. J., Bresnahan, J. C., Shuman, S. L., Masters, J. N., & Beattie, M. S. (1997). Apoptosis and delayed degeneration after spinal cord injury in rats and monkeys. *Nature Medicine*, *3*, 73–76. https://doi.org/10.1038/nm0197-73

DeWitt, I., & Rauschecker, J. P. (2013). Wernicke's area revisited: Parallel streams and word processing. *Brain and Language*, *127*, 181–191. https://doi.org/10.1016/j.bandl.2013.09.014

Diaz-de-Grenu, L. Z., Acosta-Cabronero, J., Pereira, J. M. S., Pengas, G., Williams, G. B., & Nestor, P. J. (2011). MRI detection of tissue pathology beyond atrophy in Alzheimer's disease: Introducing T2-VBM. *NeuroImage*, *56*, 1946–1953. https://doi.org/10.1016/j.neuroimage.2011.03.082

Dick, A. S., & Tremblay, P. (2012). Beyond the arcuate fasciculus: Consensus and controversy in the connectional anatomy of language. *Brain*, *135*, 3529–3550. https://doi.org/10.1093/brain/aws222

Dronkers, N. F., Plaisant, O., Iba-Zizen, M. T., & Cabanis, E. A. (2007). Paul Broca's historic cases: High resolution MR imaging of the brains of Leborgne and Lelong. *Brain*, *130*, 1432–1441. https://doi.org/10.1093/brain/awm042

Duffau, H. (2013). A new philosophy in surgery for diffuse low-grade glioma (DLGG): Oncological and functional outcomes. *Neurochirurgie*, *59*, 2–8. https://doi.org/10.1016/j.neuchi.2012.11.001

Duffau, H. (2015). Stimulation mapping of white matter tracts to study brain functional connectivity. *Nature Reviews. Neurology*, *11*, 255–265. https://doi.org/10.1038/nrneurol.2015.51

Fridriksson, J., den Ouden, D. B., Hillis, A. E., Hickok, G., Rorden, C., Basilakos, A., Yourganov, G., & Bonilha, L. (2018). Anatomy of aphasia revisited. *Brain*, *141*, 848–862. https://doi.org/10.1093/brain/awx363

Friederici, A. D. (2015). White-matter pathways for speech and language processing. *Handbook of Clinical Neurology*, *129*, 177–186. https://doi.org/10.1016/B978-0-444-62630-1.00010-X

Gaillard, R., Naccache, L., Pinel, P., Clémenceau, S., Volle, E., Hasboun, D., Dupont, S., Baulac, M., Dehaene, S., Adam, C., & Cohen, L. (2006). Direct intracranial, FMRI, and lesion evidence for the causal role of left inferotemporal cortex in reading. *Neuron*, *50*, 191–204. https://doi.org/10.1016/j.neuron.2006.03.031

Ge, J., Peng, G., Lyu, B., Wang, Y., Zhuo, Y., Niu, Z., Tan, L. H., Leff, A. P., & Gao, J. H. (2015). Cross-language differences in the brain network subserving intelligible speech. *Proceedings of the National Academy of Sciences of the United States of America*, *112*, 2972–2977. https://doi.org/10.1073/pnas.1416000112

Glasser, M. F., & Rilling, J. K. (2008). DTI tractography of the human brain's language pathways. *Cerebral Cortex*, *18*, 2471–2482. https://doi.org/10.1093/cercor/bhn011

Goodale, M. A., & Milner, A. D. (1992). Separate visual pathways for perception and action. *Trends in Neurosciences*, *15*, 20–25. https://doi.org/10.1016/0166-2236(92)90344-8

Gorno-Tempini, M. L., Brambati, S. M., Ginex, V., Ogar, J., Dronkers, N. F., Marcone, A., Perani, D., Garibotto, V., Cappa, S. F., & Miller, B. L. (2008). The logopenic/phonological variant of primary progressive aphasia. *Neurology*, *71*, 1227–1234. https://doi.org/10.1212/01.wnl.0000320506.79811.da

Hickok, G., & Poeppel, D. (2004). Dorsal and ventral streams: A framework for understanding aspects of the functional anatomy of language. *Cognition*, *92*, 67–99. https://doi.org/10.1016/j.cognition.2003.10.011

Hickok, G., & Poeppel, D. (2007). The cortical organization of speech processing. *Nature Reviews. Neuroscience*, *8*, 393–402. https://doi.org/10.1038/nrn2113

Hill, A. B. (1965). The environment and disease: Association or causation? *Proceedings of the Royal Society of Medicine*, *58*, 295–300. https://doi.org/10.1177/003591576505800503

Ivanova, M. V., Isaev, D. Y., Dragoy, O. V., Akinina, Y. S., Petrushevskiy, A. G., Fedina, O. N., Shklovsky, V. M., & Dronkers, N. F. (2016). Diffusion-tensor imaging of major white matter tracts and their role in language processing in aphasia. *Cortex*, *85*, 165–181. https://doi.org/10.1016/j.cortex.2016.04.019

Jose, P. E. (2016). The merits of using longitudinal mediation. *Educational Psychologist*, *51*, 331–341. https://doi.org/10.1080/00461520.2016.1207175

Latini, F., Mårtensson, J., Larsson, E. M., Fredrikson, M., Åhs, F., Hjortberg, M., Aldskogius, H., & Ryttlefors, M. (2017). Segmentation of the inferior longitudinal fasciculus in the human brain: A white matter dissection and diffusion tensor tractography study. *Brain Research*, *1675*, 102–115. https://doi.org/10.1016/j.brainres.2017.09.005

Legland, D., Kiêu, K., & Devaux, M.-F. (2011). Computation of Minkowski measures on 2D and 3D binary images. *Image Analysis & Stereology*, *26*, 83-92. https://doi.org/10.5566/ias.v26.p83-92

Lichteim, L. (1885). On aphasia. *Brain*, *7*, 433–484. https://doi.org/10.1093/brain/7.4.433

Lindig, T., Kotikalapudi, R., Schweikardt, D., Martin, P., Bender, F., Klose, U., Ernemann, U., Focke, N. K., & Bender, B. (2018). Evaluation of multimodal segmentation based on 3D T1-, T2- and FLAIR-weighted images—The difficulty of choosing. *NeuroImage*, *170*, 210–221. https://doi.org/10.1016/j.neuroimage.2017.02.016

Mah, Y. H., Husain, M., Rees, G., & Nachev, P. (2014). Human brain lesion-deficit inference remapped. *Brain*, *137*, 2522–2531. https://doi.org/10.1093/brain/awu164

Margulies, D. S., & Petrides, M. (2013). Distinct parietal and temporal connectivity profiles of ventrolateral frontal areas involved in language production. *The Journal of Neuroscience*, *33*, 16846–16852. https://doi.org/10.1523/jneurosci.2259-13.2013

Martino, J., de Witt Hamer, P. C., Berger, M. S., Lawton, M. T., Arnold, C. M., de Lucas, E. M., & Duffau, H. (2013). Analysis of the subcomponents and cortical terminations of the perisylvian superior longitudinal fasciculus: A fiber dissection and DTI tractography study. *Brain Structure & Function*, *218*, 105–121. https://doi.org/10.1007/s00429-012-0386-5

Matchin, W., & Hickok, G. (2019). The cortical organization of syntax. *Cerebral Cortex*, *30*, 1481–1498. https://doi.org/10.1093/cercor/bhz180

Miglioretti, D. L., & Boatman, D. (2003). Modeling variability in cortical representations of human complex sound perception. *Experimental Brain Research*, *153*, 382–387. https://doi.org/10.1007/s00221-003-1703-2

Mishkin, M., Ungerleider, L. G., & Macko, K. A. (1983). Object vision and spatial vision: Two cortical pathways. *Trends in Neurosciences*, *6*, 414–417.

Nobre, A. C., Allison, T., & McCarthy, G. (1994). Word recognition in the human inferior temporal lobe. *Nature*, *372*, 260–263. https://doi.org/10.1038/372260a0

Pangman, V. C., Sloan, J., & Guse, L. (2000). An examination of psychometric properties of the mini-mental state examination and the standardized mini-mental state examination: Implications for clinical practice. *Applied Nursing Research*, *13*, 209–213. https://doi.org/10.1053/apnr.2000.9231

Price, C. J. (2012). A review and synthesis of the first 20 years of PET and fMRI studies of heard speech, spoken language and reading. *NeuroImage*, *62*, 816–847. https://doi.org/10.1016/j.neuroimage.2012.04.062

Rauschecker, J. P., & Scott, S. K. (2009). Maps and streams in the auditory cortex: Nonhuman primates illuminate human speech processing. *Nature Neuroscience*, *12*, 718–724. https://doi.org/10.1038/nn.2331

Rauschecker, J. P., & Tian, B. (2000). Mechanisms and streams for processing of "what" and "where" in auditory cortex. *Proceedings of the National Academy of Sciences of the United States of America*, *97*, 11800–11806. https://doi.org/10.1073/pnas.97.22.11800

Rilling, J. K. (2014). Comparative primate neurobiology and the evolution of brain language systems. *Current Opinion in Neurobiology*, *28*, 10–14. https://doi.org/10.1016/j.conb.2014.04.002

Rilling, J. K., Glasser, M. F., Preuss, T. M., Ma, X., Zhao, T., Hu, X., & Behrens, T. E. J. (2008). The evolution of the arcuate fasciculus revealed with comparative DTI. *Nature Neuroscience*, *11*, 426–428. https://doi.org/10.1038/nn2072

Rohrer, J. D., Ridgway, G. R., Crutch, S. J., Hailstone, J., Goll, J. C., Clarkson, M. J., Mead, S., Beck, J., Mummery, C., Ourselin, S.,

Warrington, E. K., Rossor, M. N., & Warren, J. D. (2010). Progressive logopenic/phonological aphasia: Erosion of the language network. *NeuroImage*, *49*, 984–993. https://doi.org/10.1016/j.neuroimage.2009.08.002

Rolls, E. T. (2012). Invariant visual object and face recognition: Neural and computational bases, and a model, VisNet. *Frontiers in Computational Neuroscience*, *6*, 35. https://doi.org/10.3389/fncom.2012.00035

Rosenthal, R., Cooper, H., & Hedges, L. (1994). Parametric measures of effect size. In *The handbook of research synthesis*. Russell Sage Foundation. (pp. 231–244).

Safar, M. H., & Shahabi, C. (2003). *Shape analysis and retrieval of multimedia objects*. Kluwer Academic Publishers.

Sarubbo, S., Tate, M., de Benedictis, A., Merler, S., Moritz-Gasser, S., Herbet, G., & Duffau, H. (2019). Mapping critical cortical hubs and white matter pathways by direct electrical stimulation: An original functional atlas of the human brain. *NeuroImage*, 205, 116237. https://doi.org/10.1016/j.neuroimage.2019.116237

Saur, D., Kreher, B. W., Schnell, S., Kümmerer, D., Kellmeyer, P., Vry, M. S., Umarova, R., Musso, M., Glauche, V., Abel, S., Huber, W., Rijntjes, M., Hennig, J., & Weiller, C. (2008). Ventral and dorsal pathways for language. *Proceedings of the National Academy of Sciences of the United States of America*, *105*, 18035–18040. https://doi.org/10.1073/pnas.0805234105

Trimmel, K., van Graan, A. L., Caciagli, L., Haag, A., Koepp, M. J., Thompson, P. J., & Duncan, J. S. (2018). Left temporal lobe language network connectivity in temporal lobe epilepsy. *Brain*, *141*, 2406–2418. https://doi.org/10.1093/brain/awy164

Turkeltaub, P. E., Gareau, L., Flowers, D. L., Zeffiro, T. A., & Eden, G. F. (2003). Development of neural mechanisms for reading. *Nature Neuroscience*, *6*, 767–773. https://doi.org/10.1038/nn1065

Tusa, R. J., & Ungerleider, L. G. (1985). The inferior longitudinal fasciculus: A reexamination in humans and monkeys. *Annals of Neurology*, *18*, 583–591. https://doi.org/10.1002/ana.410180512

Tzourio-Mazoyer, N., Landeau, B., Papathanassiou, D., Crivello, F., Etard, O., Delcroix, N., Mazoyer, B., & Joliot, M. (2002). Automated anatomical labeling of activations in SPM using a macroscopic anatomical parcellation of the MNI MRI single-subject brain. *NeuroImage*, *15*, 273–289. https://doi.org/10.1006/nimg.2001.0978

Wakana, S., Caprihan, A., Panzenboeck, M. M., Fallon, J. H., Perry, M., Gollub, R. L., Hua, K., Zhang, J., Jiang, H., Dubey, P., Blitz, A., van Zijl, P., & Mori, S. (2007). Reproducibility of quantitative tractography methods applied to cerebral white matter. *NeuroImage*, *36*, 630–644. https://doi.org/10.1016/j.neuroimage.2007.02.049

Wen, P. Y., Macdonald, D. R., Reardon, D. A., Cloughesy, T. F., Sorensen, A. G., Galanis, E., DeGroot, J., Wick, W., Gilbert, M. R., Lassman, A. B., Tsien, C., Mikkelsen, T., Wong, E. T., Chamberlain, M. C., Stupp, R., Lamborn, K. R., Vogelbaum, M. A., van den Bent, M. J., & Chang, S. M. (2010). Updated response assessment criteria for high-grade gliomas: Response assessment in neuro-oncology working group. *Journal of Clinical Oncology: Official Journal of the American Society of Clinical Oncology*, *28*, 1963–1972. https://doi.org/10.1200/JCO.2009.26.3541

Wilson, S. M., Bautista, A., & McCarron, A. (2018). Convergence of spoken and written language processing in the superior temporal sulcus. *NeuroImage*, *171*, 62–74. https://doi.org/10.1016/j.neuroimage.2017.12.068

Wilson, S. M., Galantucci, S., Tartaglia, M. C., Rising, K., Patterson, D. K., Henry, M. L., Ogar, J. M., DeLeon, J., Miller, B. L., & Gorno-Tempini, M. L. (2011). Syntactic processing depends on dorsal language tracts. *Neuron*, *72*, 397–403. https://doi.org/10.1016/j.neuron.2011.09.014

Woolrich, M. W., Jbabdi, S., Patenaude, B., Chappell, M., Makni, S., Behrens, T., Beckmann, C., Jenkinson, M., & Smith, S. M. (2009). Bayesian analysis of neuroimaging data in FSL. *NeuroImage*, *45*, S173–S186. https://doi.org/10.1016/j.neuroimage.2008.10.055

Yeh, F. C., Verstynen, T. D., Wang, Y., Fernandez-Miranda, J. C., & Tseng, W. Y. (2013). Deterministic diffusion fiber tracking improved by quantitative anisotropy. *PLoS One*, *8*, e80713. https://doi.org/10.1371/journal.pone.0080713

Yi, H. G., Leonard, M. K., & Chang, E. F. (2019). The encoding of speech sounds in the superior temporal gyrus. *Neuron*, *102*, 1096–1110. https://doi.org/10.1016/j.neuron.2019.04.023

Zaccarella, E., Schell, M., & Friederici, A. D. (2017). Reviewing the functional basis of the syntactic merge mechanism for language: A coordinate-based activation likelihood estimation meta-analysis. *Neuroscience and Biobehavioral Reviews*, *80*, 646–656. https://doi.org/10.1016/j.neubiorev.2017.06.011

Zhu, Y., Xu, M., Lu, J., Hu, J., Kwok, V. P. Y., Zhou, Y., Yuan, D., Wu, B., Zhang, J., Wu, J., & Tan, L. H. (2022). Distinct spatiotemporal patterns of syntactic and semantic processing in human inferior frontal gyrus. *Nature Human Behaviour*, *6*, 1104–1111. https://doi.org/10.1038/s41562-022-01334-6

SUPPORTING INFORMATION

Additional supporting information can be found online in the Supporting Information section at the end of this article.

How to cite this article: Zhang, J., Yao, Y., Wu, J., Rolls, E. T., Sun, C., Bu, L., Lu, J., Lin, C., Feng, J., Mao, Y., & Zhou, L. (2023). The cortical regions and white matter tracts underlying auditory comprehension in patients with primary brain tumor. *Human Brain Mapping*, *44*(4), 1603–1616. https://doi.org/10.1002/hbm.26161